

## Laser Location and Manipulation of a Single Quantum Tunneling Channel in an InAs Quantum Dot

O. Makarovskiy,<sup>1</sup> E. E. Vdovin,<sup>1,2</sup> A. Patané,<sup>1</sup> L. Eaves,<sup>1,\*</sup> M. N. Makhonin,<sup>3</sup> A. I. Tartakovskii,<sup>3</sup> and M. Hopkinson<sup>4</sup>

<sup>1</sup>*School of Physics and Astronomy, The University of Nottingham, NG7 2RD, United Kingdom*

<sup>2</sup>*Institute of Microelectronics Technology RAS, 142432 Chernogolovka, Russia*

<sup>3</sup>*Department of Physics and Astronomy, University of Sheffield, Sheffield S3 3JD, United Kingdom*

<sup>4</sup>*Department of Electronic and Electrical Engineering, University of Sheffield, Sheffield S3 3JD, United Kingdom*

(Received 13 September 2011; published 14 March 2012)

We use a femtowatt focused laser beam to locate and manipulate a single quantum tunneling channel associated with an individual InAs quantum dot within an ensemble of dots. The intensity of the directed laser beam tunes the tunneling current through the targeted dot with an effective optical gain of  $10^7$  and modifies the curvature of the dot's confining potential and the spatial extent of its ground state electron eigenfunction. These observations are explained by the effect of photoexcited hole charges which become bound close to the targeted dot, thus acting as an optically induced gate electrode.

DOI: 10.1103/PhysRevLett.108.117402

PACS numbers: 78.67.Hc, 73.40.Gk, 73.50.Pz, 73.63.Kv

Several optoelectronic device concepts in emerging nanotechnologies exploit the electrical injection of charge carriers into a single, discrete quantum state and the control of this process by an external field [1–5]. Although the manipulation of a single quantum state is technically challenging, progress has been made in locating individual quantum states [4–6], controlling their interaction with the environment [4,5,7], and fine-tuning their properties [8,9] with a view to applications in photonics and quantum information [10,11]. In this Letter we describe an optical technique that uses a focused laser beam to address and manipulate a single quantum state within an ensemble of self-assembled InAs quantum dots (QDs).

Our device is a heterostructure tunnel diode containing a single layer of InAs dots in the tunnel barrier. Over a particular range of bias the measured current arises from resonant tunneling of electrons through a single QD eigenstate. We locate the spatial position of this state at micron-scale resolution by scanning the focused laser beam over the surface of the diode and measuring the effect of the photoexcited carriers on the resonant tunneling current channel. By directing the laser beam onto a particular dot we can switch the current tunneling through the dot using laser powers as low as 2 fW with an on/off ratio  $>50$  and an effective optical gain of  $\sim 4 \times 10^6$ . These phenomena arise from the Coulomb interactions between the tunneling electron and photoexcited holes which become bound within a few tens of nanometers of the active dot, thus acting like an optically induced gate electrode [12]. The optical excitation can be used to manipulate the confining potential so that the bound holes not only lower the Coulomb potential energy of the dot eigenstate, but also modify the curvature of the confinement potential as revealed by magnetotunneling imaging of the electronic eigenfunction. This experimental demonstration of laser location and optical control of resonant tunneling through a

single quantum state advances the science of quantum dot manipulation and the prospect of future applications, including sensitive photon detection.

Our diodes, shown schematically in Fig. 1(a), were grown by molecular beam epitaxy on a (001)-oriented Si-doped GaAs substrate. A single layer of self-assembled

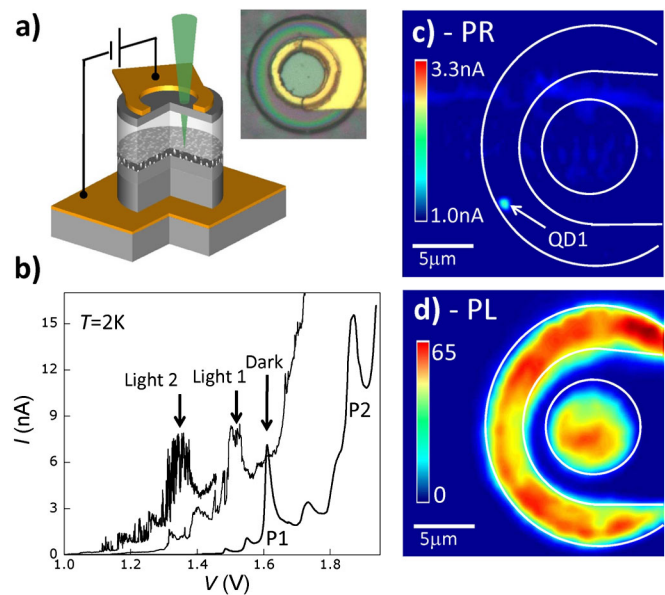


FIG. 1 (color online). (a) Sketch of the  $n$ - $i$ - $n$  resonant tunnel diode with a layer of QDs inside an (AlGa)As barrier in the intrinsic  $i$  region. Inset: Photograph of the diode surface. (b)  $I(V)$  curves at  $T = 4$  K in the dark and under illumination with an unfocused laser beam (Light 1:  $P = 3$  nW; Light 2:  $P = 8$  nW). (c) Photoresponse map at  $V = 1.35$  V measured under illumination with a focused laser beam ( $P = 2$  fW,  $T = 4$  K,  $d_L < 1$  μm). (d)  $\mu$ PL map of the QD emission at  $\lambda = 905$  nm ( $P = 1$  μW,  $T = 4$  K,  $d_L < 1$  μm).

InAs QDs with sheet density  $n_{\text{QD}} = 2.0 \pm 0.5 \times 10^{15} \text{ m}^{-2}$  is embedded in the central plane of an 8 nm  $\text{Al}_{0.4}\text{Ga}_{0.6}\text{As}$  tunnel barrier [13]. The continuum of states of the InAs wetting layer to the right of the barrier facilitates electron tunnelling out of the dots. The active layer of the device is sandwiched between two heavily doped  $n^+$  GaAs layers. To enhance the optical sensitivity of our device, we have incorporated a layer of undoped GaAs of thickness  $t = 0.5 \mu\text{m}$  directly below the top contact layer. This layer is thick enough to absorb a significant fraction ( $> 20\%$ ) of the above band gap excitation light incident on the mesa diode. The structures were processed into optical mesa diodes of  $25 \mu\text{m}$  diameter. A small central circular contact and an outer ring-shaped contact formed by an annealed AuGe/Ni/Au layer provide optical access to the top surface of the diode.

For the spatially resolved photoresponse and photoluminescence (PL) measurements, we used a confocal microscope spectrometer equipped with a microscope cryostat or a He-bath cryostat incorporating a XYZ stage and focusing microlens. Optical excitation was provided by a focused He-Ne laser beam with spot diameter  $d_L < 1 \mu\text{m}$  and power  $P$  down to 2 fW. We performed current-voltage,  $I(V)$ , measurements with the device mounted inside a superconducting magnetocryostat at fields  $B$  up to 14 T. Magnetotransport experiments were performed in darkness and with the top surface of the device uniformly illuminated by an unfocused 633 nm He-Ne laser beam ( $P < 10 \text{ nW}$ , spot diameter  $d_L > 1 \text{ mm}$ ).

The sharp resonant peaks in the “dark”  $I(V)$  curve at low temperature ( $T = 4 \text{ K}$ ) have amplitudes,  $I_r$ , of several nA [Fig. 1(b)]. We have performed a detailed study of their temperature dependence which indicates that they arise from electron tunneling out of the Fermi sea in the GaAs emitter through individual, discrete QD states in the tunnel barrier (see Supplemental Material [14], Fig. S2). The voltage width of each resonance ( $\sim 40 \text{ mV}$ ) corresponds to an energy range of  $\sim 4 \text{ meV}$  for the electrons tunneling into the QD. This takes account of the electrostatic leverage factor [15] of our device which we estimate to be  $f = 11$  from the temperature dependent measurements (see Supplemental Material [14], Fig. S2).

When the upper surface of the diode is illuminated uniformly with unfocused laser light of increasing intensity, the QD resonant peaks shift steadily towards lower bias [16]. However, the shapes, amplitudes, and relative bias positions of the peaks remain approximately the same. The shifts to lower bias,  $\Delta V$ , are proportional to the light intensity at low levels, but saturate to about 300 mV at a light intensity  $P \approx 1 \mu\text{W}/\text{cm}^2$ . The response of the diode to illumination is shown in Fig. 1(c) as a color map of the photoresponse (PR), which we obtain by scanning a focused low intensity laser beam ( $P = 2 \text{ fW}$  or  $\sim 200 \text{ nW}/\text{cm}^2$ ) over the top surface and measuring the tunnel current at each position for a fixed applied bias. The

map reveals a strong response from a microscopic “hot spot.” In contrast, the map of the open circuit microphotoluminescence ( $\mu\text{PL}$ ) measured with the same scanned laser beam shows a more uniformly distributed PL signal [Fig. 1(d)]. The PL emission is dominated by a broad band centered at a photon energy of 1.38 eV and full width at half maximum of 70 meV due to electron-hole recombination within the QDs.

The photoexcitation of a particular hot spot in the photoresponse map produces a characteristic change in  $I(V)$ . As shown in Figs. 2(a) and 2(b), when the laser is focussed on the QD1 hot spot, peak P1 shifts to lower bias (1.5 V) whereas, on the QD2 spot, peak P2 shifts but peak P1 remains fixed. By measuring the relative changes of the peak currents,  $I_r$  [Figs. 2(c) and 2(e)] or of the voltage shifts  $\Delta V$  [Figs. 2(d) and 2(f)] of the selected resonances as a function of the  $xy$  coordinates around QD1 and QD2, we obtain a characteristic spot radius of  $\sim 2 \mu\text{m}$ .

With uniform illumination, the light-induced voltage shift is accompanied by temporal fluctuations in the tunnel

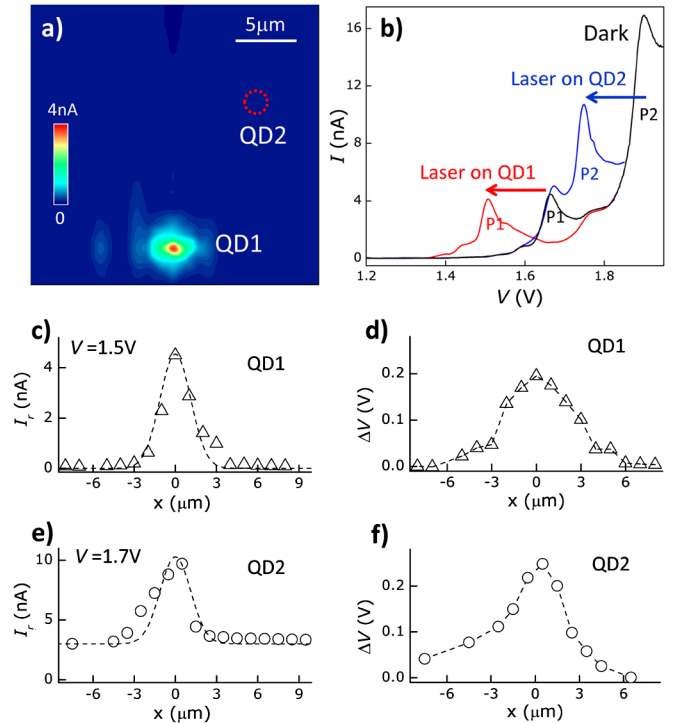


FIG. 2 (color online). (a) Photoresponse map measured at  $V = 1.5 \text{ V}$  showing “hot spot” region QD1. The red circle indicates the position of a second hot spot (QD2). (b)  $I(V)$  curves in the dark and under illumination of the QD1 and QD2 spots. Arrows indicate light-induced shifts of the QD resonances for QD1 (red) and QD2 (blue). (c) and (e) Spatial profiles of the photoresponse across the QD1 and QD2 spots measured at 1.5 V and 1.7 V, respectively. The dashed lines are guides to the eye. (d) and (f) Bias shifts of the QD1 and QD2 resonances as a function of the laser spot distance from the centers of the QD1 and QD2 spots.

current, which generates noise when the  $I(V)$  curves are acquired at slow sweep rates ( $< 1$  Hz) [Fig. 1(b)]. This jitter is attributed to slow fluctuations in current paths between the contact layers and barrier and it can be eliminated by making fast ( $< 0.1$  s) sweeps of  $I(V)$  [16]. However, with the low power (2 fW) scanned and focused laser beam, the data remain noise-free [Fig. 2(b)] and the resonant current is stable for a time  $\tau_s \sim 10$  s, which is sufficient time to acquire noise-free  $I(V)$  plots using conventional dc measurement techniques.

The scanning experiments with the focused laser beam demonstrate that we can address a particular QD tunneling channel [e.g., peak QD1 in Fig. 1(b)] and tune or detune the resonance by changing either the bias or the laser beam intensity. We attribute the bias-induced shift of the QD resonance to the mechanism illustrated schematically in Fig. 3(a). Under illumination, the photoexcited electrons drift towards the positively biased top  $n^+$ GaAs contact layer and have no significant effect on the behavior of the device. Photoexcited holes created in the undoped GaAs layer below the top contact drift towards the tunnel barrier due to the action of the electric field generated by the applied bias. The wetting layer to the right of the tunnel barrier captures the holes which can then tunnel into the long lived ( $\sim 1$  sec) bound states in the QD layer. Those holes which become bound close to an active dot, e.g., QD1, create a ‘‘hot spot’’ by lowering the local electrostatic potential for tunneling electrons, thus reducing the value of the applied bias required for resonant tunneling. Using Gauss’s theorem, we can use the light-induced shift in bias to estimate the areal density of holes,  $n_h$ , bound in the region of the QD layer, i.e.,  $\Delta V = -n_h e t / \epsilon_0 \epsilon_r$ , giving  $n_h = 4 \times 10^{14} \text{ m}^{-2} \sim 0.2 n_{\text{QD}}$  when the bias shift saturates at high optical excitation. Thus a significant fraction of the QDs can be charged with holes.

The positive charge of the photoexcited holes bound close to the active dot serves as an optically controlled, microscopic gate electrode which can switch the resonant tunnel current with a high degree of fidelity (on/off ratio  $> 50$ ). We emphasize that the effect can be achieved with laser powers  $P$  as low as 2 fW, which corresponds to a photo-hole generation rate in the light-absorbing GaAs layer of only  $\sim 2000 \text{ s}^{-1}$ . The electron resonant tunneling rate through an active dot is 7 orders of magnitude larger than this. Hence the contribution to the resonant current of electron recombination with the photoexcited holes within the active quantum dot is negligible. The corresponding optical gain is  $\eta = \frac{I_{\text{ph}} h\nu}{P_e} \sim 4 \times 10^6$ , where  $h\nu$  is the photon energy. The high photosensitivity of our device indicates a long dwell time ( $\tau_d > 1$  s) of a photoexcited hole following capture at one of the dots. This optical memory can be erased by applying a reverse bias pulse, which quickly sweeps out the bound holes. The dot is then reactivated for photon detection.

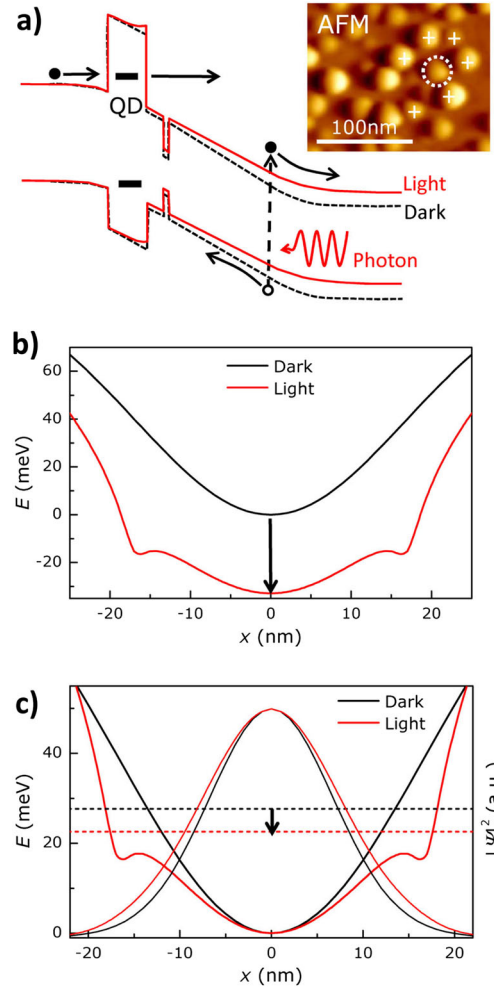


FIG. 3 (color online). (a) Sketch of electron tunneling from the  $n$ -GaAs emitter layer into the energy level of a QD in the dark (dashed lines) and in the presence of photoexcited electron-hole pairs (solid lines). The inset shows the atomic force microscopy (AFM) image of the InAs QDs illustrating several bound holes (+) surrounding an active QD (circled). (b) Calculated average energy potential in the dark and under illumination for a QD surrounded by positive charges. (c) Model calculation of the average potential energies and corresponding electron wave function probability densities (ground state) in the dark and under illumination. The plane of the bound photoexcited holes is offset by 1 nm from the calculated potential plane. The arrows in parts (b) and (c) show the shift of the potential energy (b) and of the corresponding ground state (c) caused by light.

To examine how the bound holes modify the electronic eigenstate of the active quantum dot QD1, we measured the effect of an applied magnetic field on the resonant tunneling current, as shown in Fig. 4(a). The field was applied in the  $x$ - $y$  plane, perpendicular to the direction of the current flow. We attribute the noise in the resonant peaks to random variations in the electrostatic potential associated with the changing spatial configuration of the nearby photoexcited bound holes which have a

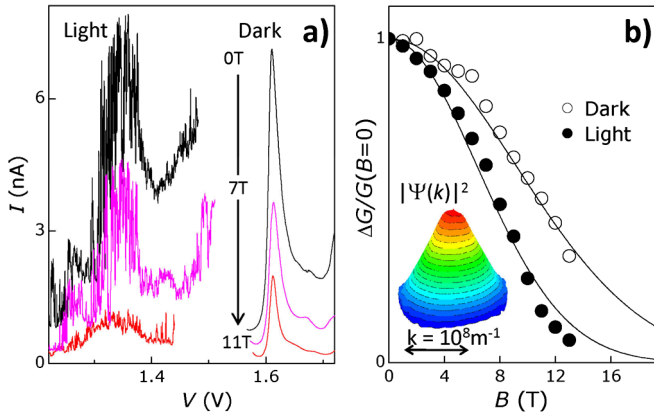


FIG. 4 (color online). (a)  $I(V)$  plots in the bias region of the QD1 resonance at magnetic fields  $B = 0, 7$  T, and  $11$  T applied perpendicular to the current in the dark and under illumination ( $T = 2$  K). (b)  $B$  dependence of the differential conductance of the QD1 peak in the dark and under illumination. Solid lines are Gaussian fits of the data. Inset: Electron probability density  $|\Psi|^2$  in  $k$  space for the QD1 ground state measured in the dark.

characteristic lifetime of  $\sim 1$  s. The  $I(V)$  curves under illumination were measured over a time period of  $>10^3$  sec and therefore correspond to a time average of the light-induced change in the confinement potential of the active dot.

When an electron tunnels from the emitter into the QD eigenstate, it acquires an additional in-plane momentum from the Lorentz force given by  $\hbar k_y = -eB_x s$ , where  $s$  is the effective tunneling length along  $z$ . By measuring the tunnel current as a function of  $B_x (\propto k_y)$ , we determine the electron probability density in momentum space of the eigenstate, i.e.,  $I(B_x) \sim |\Psi(k_y)|^2$  [15]. The decrease in the amplitude of the QD1 resonance with increasing  $B$  is more pronounced when the device is illuminated [see Fig. 4(b)]. This corresponds to an increase, under illumination, of the spatial extent of the ground state eigenfunction in real space. We attribute this behavior to the effect of the photoexcited holes which become bound close ( $\sim 20$  nm) to the active dot. The attractive Coulomb forces exerted by the bound holes act to soften the curvature of the confining potential of the active dot, thus increasing the spatial extent of its electronic eigenfunction.

We model this effect by approximating the in-plane confinement of the QD by a two-dimensional potential  $U = -U_0 \exp(-r^2/a^2)$ . The parabolic curvature of this potential close to its minimum is characterized by a quantization energy  $\hbar\omega_0$ , where  $\omega_0 = \sqrt{2U_0 m^*/a^2}$  and  $m^* = 0.03m_e$  is the electron effective mass for the InAs dot. Figures 3(b) and 3(c) show the changes in the confining potential and the corresponding ground state probability density when a hole is placed on each of the  $N$  neighboring dots surrounding an empty active dot. For simplicity, we locate the holes at equal spacings on a circle of radius  $d$

centered on the active dot. For the calculations shown in Figs. 3(b) and 3(c), we use  $\hbar\omega_0 = 30$  meV,  $U_0 = 100$  meV,  $N = 6$ , and  $d = 17$  nm and include the effect of the image charges of the bound holes due to the nearby conducting  $n$ -GaAs contact layers ([17], see also Supplemental Material [14] for further details). For these parameter values, our simple model predicts that the nearby hole charges increase the FWHM of the ground state probability density by 12%, which is in qualitative agreement with the measured value  $17 \pm 5\%$ , see Fig. 4(b). Previous imaging studies of the electron bound to InAs dots [18,19] or to Si-donors in a quantum well [20] have demonstrated that a strong magnetic field applied perpendicular to the plane of the dots (or to the quantum well plane) leads to the magnetocompression of the electron eigenfunction in real space. Here we have demonstrated that a different type of external perturbation, namely, the Coulomb attraction of bound photoexcited holes can produce a significant and measurable increase in the spatial extent of the ground state eigenfunction of a QD.

In summary, we have demonstrated a high resolution photoconductivity mapping technique whereby a single quantum dot within a large ensemble of dots can be optically activated and tuned by scanning a focused laser beam over the top surface of a tunnel diode. The laser light generates photoexcited holes which become bound in the vicinity of the active dot; this changes not only the electrostatic potential energy of the dot making it electrically active, but also the curvature of its confining potential. This optical tuning of the confining potential is confirmed by measuring the photoinduced change in the spatial form of the wave function of the resonant eigenstate using magnetotunneling spectroscopy. The positively charged photoexcited holes act as a moveable optically controlled, and electrically erasable gate electrode which can switch the resonant tunneling current through a targeted dot with an on/off ratio  $> 50$  at optical excitation levels as low as 2 fW. This could be used to develop sensitive photon detectors and to advance existing methods for the controlled manipulation of single quantum states in nanoscale optoelectronic devices.

This work was supported by The Leverhulme Trust, the Royal Society (UK), and the Engineering and Physical Sciences Research Council (UK). One of the authors (E.V.) acknowledges financial support from RFBR (Russia). We are grateful to Professor Maurice Skolnick for helpful advice and discussion.

\*Corresponding author

Laurence.Eaves@nottingham.ac.uk

- [1] Z. Yuan, B. E. Kardynal, R. M. Stevenson, A. J. Shields, C. J. Lobo, K. Cooper, N. S. Beattie, D. A. Ritchie, and M. Pepper, *Science* **295**, 102 (2002).

- [2] C. L. Salter, R. M. Stevenson, I. Farrer, C. A. Nicoll, D. A. Ritchie, and A. J. Shields, *Nature (London)* **465**, 594 (2010).
- [3] A. Gerardino, M. Francardi, A. Gaggero, F. Mattioli, R. Leoni, L. Balet, N. Chauvin, F. Marsili, and A. Fiore, *Opto-Electron. Rev.* **18**, 352 (2010).
- [4] A. J. Shields, *Nature Photon.* **1**, 215 (2007).
- [5] C. Bockler, S. Reitzenstein, C. Kistner, R. Debusmann, A. Loeffler, T. Kida, S. Hofling, A. Forchel, L. Grenouillet, J. Claudon, and J. M. Gerard, *Appl. Phys. Lett.* **92**, 091107 (2008).
- [6] K. H. Lee, A. M. Green, R. A. Taylor, D. N. Sharp, J. Scrimgeour, O. M. Roche, J. H. Na, A. F. Jarjour, A. J. Turberfield, F. S. F. Brossard, D. A. Williams, G. Andrew, and D. Briggs, *Appl. Phys. Lett.* **88**, 193106 (2006).
- [7] J. P. Reithmaier, G. Sek, A. Löffler, C. Hofmann, S. Kuhn, S. Reitzenstein, L. V. Keldysh, V. D. Kulakovskii, T. L. Reinecke, and A. Forchel, *Nature (London)* **432**, 197 (2004).
- [8] M. V. Maximov, A. F. Tsatsul'nikov, B. V. Volovik, D. S. Sizov, Yu. M. Shernyakov, I. N. Kaiander, A. E. Zhukov, A. R. Kovsh, S. S. Mikhlin, V. M. Ustinov, Zh. I. Alferov, R. Heitz, V. A. Shchukin, N. N. Ledentsov, D. Bimberg, Yu. G. Musikhin, and W. Neumann, *Phys. Rev. B* **62**, 16671 (2000).
- [9] F. Ding, R. Singh, J. D. Plumhof, T. Zander, V. Krapek, Y. H. Chen, M. Benyoucef, V. Zwiller, K. Dorr, G. Bester, A. Rastelli, and O. G. Schmidt, *Phys. Rev. Lett.* **104**, 067405 (2010).
- [10] P. M. Petroff, *Adv. Mater.* **23**, 2372 (2011).
- [11] O. Benson, C. Santori, M. Pelton, and Y. Yamamoto, *Phys. Rev. Lett.* **84**, 2513 (2000).
- [12] J. C. Blakesley, P. See, A. J. Shields, B. E. Kardynał, P. Atkinson, I. Farrer, and D. A. Ritchie, *Phys. Rev. Lett.* **94**, 067401 (2005).
- [13] The detailed layer composition in order of growth is as follows: a 1  $\mu\text{m}$  GaAs buffer layer with  $2 \times 10^{18} \text{ cm}^{-3}$  Si doping; a 40 nm undoped GaAs layer; a 4 nm undoped  $\text{Al}_{0.4}\text{Ga}_{0.6}\text{As}$  layer; a QD layer formed by 2.2 monolayers (ML) of InAs; a 4 nm undoped  $\text{Al}_{0.4}\text{Ga}_{0.6}\text{As}$  layer; a 4 nm undoped GaAs layer; a 1.2 ML InAs undoped wetting layer; a 500 nm undoped GaAs layer; a 50 nm GaAs layer with  $2 \times 10^{17} \text{ cm}^{-3}$  Si doping; and finally a 0.5  $\mu\text{m}$  GaAs layer with  $2 \times 10^{18} \text{ cm}^{-3}$  Si doping. The structures were grown at 550 °C except for the InAs layers and the layers above, which were grown at 550 °C.
- [14] See Supplemental Material at <http://link.aps.org/supplemental/10.1103/PhysRevLett.108.117402> for the schematic energy band diagram, temperature dependence of the electron tunnel current, and discussion of the model used to fit data.
- [15] A. Patanè, R. J. A. Hill, L. Eaves, P. C. Main, M. Henini, M. L. Zambrano, A. Levin, N. Mori, and C. Hamaguchi, Yu. V. Dubrovskii, E. E. Vdovin, D. G. Austing, S. Tarucha, and G. Hill, *Phys. Rev. B* **65**, 165308 (2002).
- [16] E. E. Vdovin, O. Makarovskiy, A. Patanè, L. Eaves, and Yu. N. Khanin, *Phys. Rev. B* **79**, 193311 (2009).
- [17] M. Zahn, *Am. J. Phys.* **44**, 1132 (1976).
- [18] M. Rontani, *Nature Mater.* **10**, 173 (2011).
- [19] W. Lei, C. Notthoff, J. Peng, D. Reuter, A. Wieck, G. Bester, and A. Lorke, *Phys. Rev. Lett.* **105**, 176804 (2010).
- [20] A. Patanè, N. Mori, O. Makarovskiy, L. Eaves, M. L. Zambrano, J. C. Arce, L. Dickinson, and D. K. Maude, *Phys. Rev. Lett.* **105**, 236804 (2010).